Multi-Resolution Parameterization of Meshes for Improved Surface Based Registration

Sylvain Jaume[a], Matthieu Ferrant[a], Simon Warfield[b] and Benoît Macq[a]

[a]Laboratory of Telecommunications and Remote Sensing, Université catholique de Louvain, Place du Levant, 2, B-1348 Louvain-la-Neuve, Belgium

[b]Surgical Planning Laboratory, Harvard Medical School, Boston, USA

ABSTRACT

Common problems in medical image analysis involve surface-based registration. The applications range from atlas matching to tracking an object's boundary in an image sequence, or segmenting anatomical structures out of images. Most proposed solutions are based on deformable surface algorithms. The main problem of such methods is that the local accuracy of the matching must often be traded off against global smoothness of the surface in order to reach global convergence of the deformation process. Our contribution is to first build a Multi-Resolution (M-R) surface from a reference segmented image, and then match this surface onto the target image in an M-R fashion using a deformable surface-like algorithm. As we proceed from lower to higher resolution, the smoothing effect of the deformable surface is more and more localized, and the surface gets closer and closer to the target boundary. We present initial results of our algorithm for atlas registration onto brain MRI showing improved convergence and accuracy over classical deformable surface methods.

Keywords: Multi-Resolution, Iso-Surface Extraction, Mesh, Surface Parameterization, Registration, Active-Surface

1. INTRODUCTION

A common problem in medical image analysis involves surface-based deformation algorithms for registering surfaces onto an image or another surface. The registration of a labelled reference atlas onto a target image helps the segmentation and allows the automatic labeling of these images. This is of particular interest in the segmentation of the cortical brain surface and the labeling of the sulci.[1] For boundary detection, a deformable surface aims at tracking an object's boundary in an image sequence like a real-time MRI of a beating heart.[2] Surface-based registration also allows for the quantification of anatomic differences between subjects or within the same subject over time.[3] In the study of the brain, a surface matching algorithm can quantify the structural changes due to growth and degenerative diseases.[4]

Most proposed solutions to these problems involve active surface-like methods. These methods are based on the concept of *snakes*, introduced by Kass, Witkin and Terzopoulos.[5] They define a snake as an energy-minimizing curve which is used to extract features of interest in 2D images. This curve moves through the spatial domain of an image to minimize an energy functional P derived from the image. Since this function must take its smaller values at the features of interest, the authors propose P to equal the opposite of the squared norm of the image gradient, $P = -|\nabla I|^2$. Then the external force, $F_{ext} = -\nabla P$, attracts the snake towards the detected edges in the image. The main problems with this formulation are the following. First no attraction force to the target object applies far away from the surface, this is the capture range problem. Second for stability of the deformation process the smoothness of the curve needs to be maintained. This results in less precision of the matching, thus limiting the detail capture.

Cohen and Cohen[6] generalize and improve the concept of snakes to 3D images for shape recovery. They modifiy the force F_{ext} by normalizing the associated potential force and by adding a pressure force, also called *balloon force*. This balloon force extends the capture range of the deformable surface and needs to be initialized either to inflate the deformable surface or to deflate it. On top of the external forces, internal forces F_{int} are introduced to limit the bending of the deformable surface and thus to increase the stability of the deformation. The key issue is to find a good balancing between the internal forces F_{int} and the external forces F_{ext}. To ensure a good convergence of such a surface matching method, one often needs to sacrifice local precision leading to a globally smooth and low-resolution matched surface.

Previous work in our lab[7] used this expression of active-surface to segment structures out of brain MRI. The method achieved good results to localize and identify brain structures, but there was still the problem of the detail capture prevented by the curve smoothness.

Xu and Prince[8] propose a modified expression of the attraction force field of the curve based on electromagnetics. The force deriving from this so-called *gradient vector flow* is specified as a balance force condition. This method exhibits less sensitivity to initialization and converges effectively towards boundary cavities. However the solution requires to solve a parabolic partial differential equation, which make the calculations very expensive for extension to 3D.

Davatzikos[9] proposes a deformable surface algorithm for matching the cortical surface using control points to force the curve to penetrate sharp folds. The author finds a map between corresponding cortical regions in two brain images. He then determines a 3D elastic warping transformation to bring the two images into register.

In all these methods, either a new approach to attract the surface towards the object or manual interaction is needed to achieve reasonable matching results. Leroy et al.[10] introduced Multi-Resolution active contour for boundary detection in 2D images with reduced computational costs. They start from a coarse curve they match on a subsampled image. Then they resample the image and resize the curve to carry on the matching at the following resolution. Although it provides a quick M-R representation that solves the capture range problem, subsampling the image can cause the curve to miss some details that could not be recovered in the following resolutions. Moreover the interpretation of the object shape based on the lowest resolution representations is circumvented due to the block effect of subsampling.

We propose to explore a new path for doing surface based registration: Multi-Resolution surface matching. The idea is to borrow principles from Multi-Resolution Signal Processing and to apply them to irregularly sampled and arbitrarily connected 3D surface meshes, as recently introduced by Daubechies et al[11] and Guskov et al.[12] We introduce a M-R parameterization of surfaces for automatic surface registration. We start from a coarse surface model that we match onto a target object. We locally inflate or deflate this surface depending on the image information in a similar way to Wood et al.,[13] but we apply a different smoothing. When a balance between the matching force and smoothing force is obtained, the surface is globally refined and serves as initialization for matching at the next resolution. We repeat this operation until all the image details are captured. Matching the surface from coarse to fine allows for an improved convergence and precision of the deformation process.

The paper is organized as follows. Section 2 describes how we construct a Multi-Resolution model, and how we deform it into a target image. When applied to an atlas image our parameterization and deformation model must provide as much geometric information as possible to later help the matching of this atlas onto a new image. In section 3 we report some first experimental results obtained for brain atlas matching. Section 4 discusses some improvements as well as some further potential applications of our method. Finally section 5 concludes with a summary of our algorithm.

2. DESCRIPTION OF OUR ALGORITHM

Our idea is to build a reference M-R surface that we can then match onto target scans. We do the matching in a M-R fashion with an active surface-like algorithm. As we proceed from lower to higher resolution, the smoothing effect of the active surface is more and more localized, and the surface gets closer and closer to the target boundary. We apply a local integration of the euclidean distance to this object over our surface model. Therefore our method gives smooth representations of the shape of the target object without the voxelized aspect of Marching Cubes meshes.[14]

For the surface model at resolution $i = 0$, we start with a low triangle count mesh. In this study we have limited the class of surfaces to those having spherical topology. Other extensions are of course possible. We match this coarse surface onto the object to minimize a distance measure to the target image. We allow the deformation to result in a local inflation or deflation of the surface. Then we refine the matched surface with smaller cells between the nodes and we update the deformation directions. This new surface representation serves as the initialization of the matching process at resolution $i + 1$. We iteratively carry the matching from a low resolution to a higher resolution until all details of the target image are represented in the surface model. Figure 1 gives a overview of our M-R approach for surface matching.

The Multi-Resolution Signal Processing foundations of our method come from the use of different sampling rates. The sampling of a signal obeys a fundamental law which states that the higher the sampling rate, the higher the
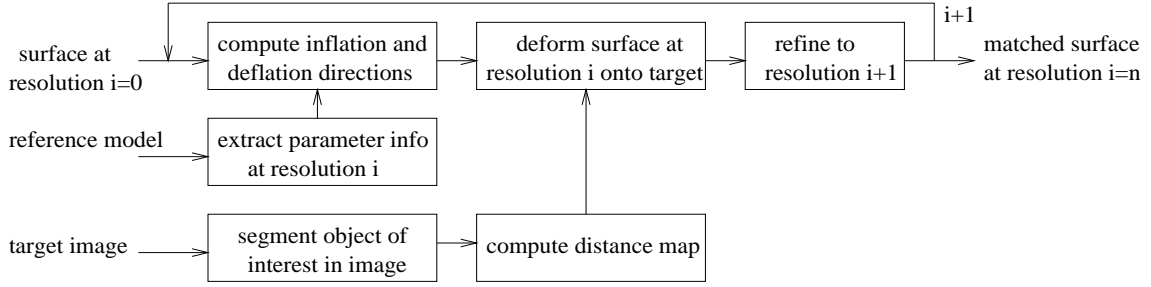
Figure 1. Block diagram of our M-R surface matching algorithm

frequencies that can be represented. If the sampling step is small enough, the discretization can capture the whole spectrum of the original signal. These concepts were generalized to 2D image analysis, with so-called Wavelets. Wavelets allow to separate different spatial discretization and frequential contents depending on the resolution. The Multi-Resolution extends this theory to irregular settings in 3D and leverages much of the mathematical foundations of Wavelets.[11] The M-R theory addresses the arbitrary geometry and connectivity of triangulated surfaces. In our approach, we refine the surface model with a smaller sampling step to localize the matching process. The deformable surface can thus capture image details that were smoothed out at the previous resolution.

2.1. Generation of a M-R Model from a Reference Image

The M-R parameterization of the meshes we use is a variation of the algorithm of Normal Meshes by Guskov et al.[15] The idea is to represent meshes starting with a low-resolution version of the original mesh with a low triangle count, and splitting each triangle by quadrisection as resolution increases. Refining the mesh by successive quadrisection generates a semi-regular mesh, where only the nodes of the coarse mesh have valence other than six. The position of the new vertices is determined by a single parameter, its distance to the higher resolution surface along surface normal. This leads to a compact and efficient M-R representation of parameterized surface meshes.

In an active surface way, we tend to minimize a potential that reflects two conflicting goals: the fitness to the original object and the smoothness of the deformable surface. Similarly to the approach of Wood et al.,[13] our fitness measure is derived from a signed distance transform of the object. Since we developed a M-R algorithm, the trade-off between fitness and smoothness is dealt with at each resolution improving the convergence.

Traditionally the image force is oriented in the gradient direction. This causes the curve to shrink close to image peaks and to expand to the closest boundaries instead of entering the cavities as figure 2 illustrates. As reported by Xu and Prince,[8] the balloon force introduced to extend the capture range does not help the surface to progress into the image cavities. Note that our approach does not suffer from a limited capture range since it starts from a coarse surface model readily approximating the target object. To progress into image cavities, we make the inflation or deflation of the surface dependent on the image. We move the surface either in the normal direction if the local region is inside the object, or in the opposite direction if outside the object. Consequently the deformable surface locally inflates or deflates to match the boundary of the target object. This encourages the surface to effectively enter the folds as the resolution increases.

Our surface model is parameterized by a node position on the surface and a scalar representing the height relative to the surface at the previous resolution. The deformation directions are thus the normals of the surface evaluated prior to deformation. Since refining the surface does not modify the surface representation, the geometry deformation from one resolution to the next is efficiently encoded in one scalar value per node.

2.2. Preserving the Regularity of the Surface Model

Similarly to active surface algorithms, we do not want incoherent deformations. We need some consistency in the neighborhood of every discretization node of the deformable surface. The M-R matching of our surface model
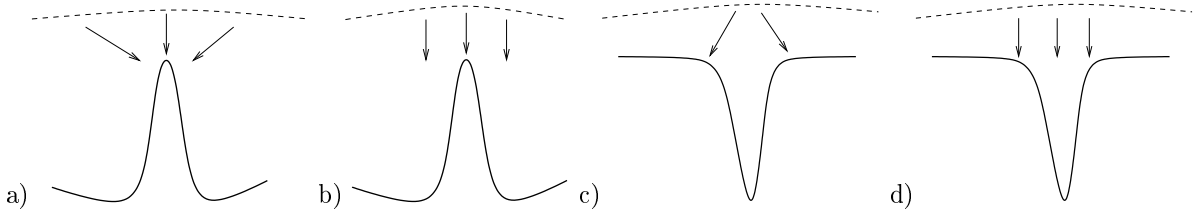
Figure 2. Directions of deformation of the contour (dashed line) near a peak in the image (bold line) when the force is oriented along (a) the image gradient or (b) the surface normal, (c-d) similar comparision in the neighborhood of an image cavity

regularly adapt the triangle size over the mesh model at each resolution. We preserve the regularity of the mesh by applying a gaussian-like smoothing of the surface nodes:

$$x_{i+1} = x_i + \lambda \sum_{j=0}^{m-1} (x_j - x_i) \tag{1}$$

where x_j are the vertices of the 1-ring neighborhood of x_i and $\lambda \in (0,1)$ is the relaxation factor. This factor must be positive and smaller than one for smoothing, otherwise the above expression results in the amplification of the local differences. As mentionned in the introduction, our surface model is based on refinements and deformations along one local axis, i.e. the normal. To keep the consistency in our model, the relaxation should occur along the normal during deformation. Therefore we only keep the component of the smoothing vector along the normal by projection onto this normal vector $\bar{n}$:

$$x'_{i+1} = x_i + (x_{i+1} - x_i).\bar{n} \tag{2}$$

To avoid instability due to large deformations, we normalize the force so that the surface nodes move by a constant time step at each iteration. We choose a time step τ of half the length of the shortest voxel edge since it is short enough to simulate a continuous path in the potential field, $\tau = min \ \{voxel\ width,\ voxel\ height,\ voxel\ depth\}$.
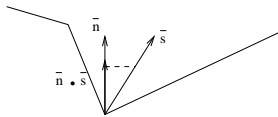
**Figure 3.** Gaussian smoothing vector $\bar{s}$ projected along local normal $\bar{n}$

2.3. Refinement of the Surface Model

Our Multi-Resolution approach is based on a refinement step each time the matching has reached equilibrium of the forces. We refine the mesh model by triangle quadrisection. The middle of the triangles edges of the mesh at resolution i are used to create the triangles of the mesh at resolution $i+1$. As depicted in figure 4 four child triangles are created from every parent triangle. Since the force is computed on local regions, the matching effect is more localized as resolution increases and the surface can capture smaller details of the image.

## 2.4. Generation of the Potential Field

Since we want to deform the surface onto the object, the potential field requires a segmented image representing this object. We apply a directional Watershed segmentation algorithm[16] based on Mathematical Morphology theory. Then we create a distance volume from the edges of the segmented object.[17] A distance volume, also called a *distance map*, is a 3D image where each voxel stores the distance to the closest edge of the segmented object. Our euclidean distance volume provides the distance from the center of every voxel to the object.

As developed in subsection 2.1, the deformation force will have a different orientation whether the surface node lies inside or outside the target object. We choose to code the inside-outside status of the voxel in the sign of
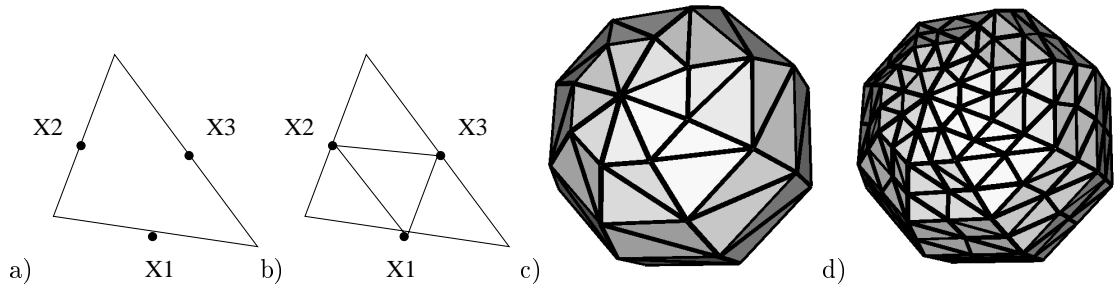
Figure 4. (a-b) Quadrisection of a triangle (c-d) refinement of the triangulated surface model of a sphere

the distance. Note that this sign is not used to compute the local distance to the object, it only serves to orient the displacement vector either in the normal direction (inflation) or in the opposite direction (deflation). This inside/outside information prevents the surface model from diverging, or to cause two bits of the surface to collapse on a single edge. This avoids the flattening of the surface when matching brains images where the folds of the cortical surface make two boundaries to be locally at equal distance from the surface.
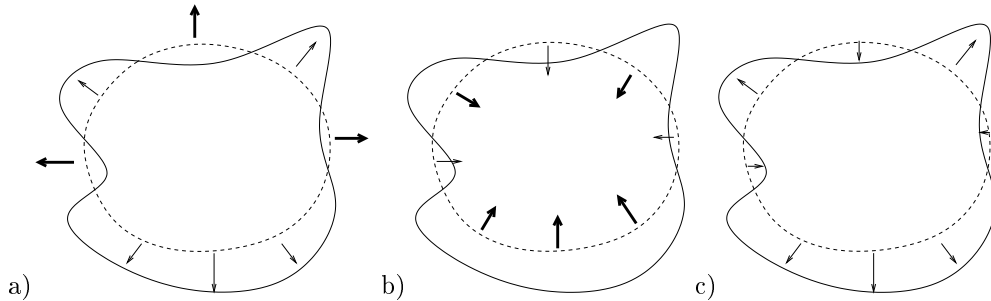
Figure 5. Deformable contour *(dash line)* and object edges *(plain line)*, bold arrows indicate forces of divergence a) balloon force initialized to point outward (inflation) b) balloon force initialized to point inward (deflation) b) making the force direction dependent on the image allows convergence irrespective of the initialization

Since we apply an inflation or deflation force depending on local image information, we do not need to define a global inflation or deflation force of our surface. Hence our deformable surface is less sensitive to a correct initialization and a precise manual intervention is not required. Figure 5 depicts the behavior of classical active surface with our approach for an initialization of the contour that crosses the object boundary. The local balloon forces that makes the surface diverge are depicted with bold arrows.

2.5. Numerical Estimation of the Distance

The local distance of the surface model to the target object (O) is evaluated at the location of every vertex x. This distance $Dist(x, O)$ is computed over the set of triangles connected to the vertex. This set of triangles is called the *1-ring neighborhood* of a vertex since all vertices connected by one edge to the center vertex belongs to it. The distance of vertex x to the object O is then

$$Dist(x, O) = \sum_{i=0}^{n-1} \frac{Area(T_i) * Dist(T_i, O)}{\sum_{j=0}^{n-1} Area(T_j)} \tag{3}$$

where T_i is a triangle connected to vertex x, and $Dist$ and $Area$ are two functions that evaluates the distance and the area respectively. This formula gives a discrete integration of the distance over the 1-ring neighborhood of a given vertex. We use a discrete integration of the distance of a triangle to the object. The approximated distance of a triangle is the weighted sum of the distance of its center and midedge points as follows

$$Dist(T, O) = \int_S Dist(x, O)dS \simeq 0.4 * Dist(x_1, O) + 0.2 * Dist(x_2, O) + 0.2 * Dist(x_3, O) + 0.2 * Dist(x_4, O) \tag{4}$$
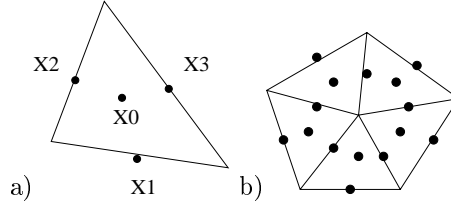
Figure 6. a) Four points where the distance is evaluated to compute the discrete integration of the distance of the triangle b) 1-ring neighborhood of a vertex

Since the euclidean distance map is a discrete 3D representation of the distance to the object, we need a function to compute a distance for any position in the continous 3D space. We choose a linear interpolation based on the values stored at the height corner vertices of a voxel. We can easily find in which voxel a given vertex in the continuous space lies in the distance map. We then compute the parametric coordinates (r, s, t) of the vertex within the voxel. The coordinate system defined by this voxel is depicted in figure 7. The distance of the vertex is then a weighted sum of surrounding values. The weights based on the parameters (r, s, t) are

$$
\begin{aligned}
w_0 &= (1-r)(1-s)(1-t) & w_4 &= (1-r)(1-s)t \\
w_1 &= r(1-s)(1-t) & w_5 &= r(1-s)t \\
w_2 &= (1-r)s(1-t) & w_6 &= (1-r)st \\
w_3 &= rs(1-t) & w_7 &= rst
\end{aligned}
\tag{5}
$$

which allow to write the distance of a vertex as the sum

$$
Dist(x, O) = \sum_{i=0}^{7} w_i * Dist(p_i, O)
\tag{6}
$$

where p_i, $0 \le i \le 7i$, represent the corner vertices of the voxel. Finally we get a scalar associated with each vertex of our mesh. This scalar is the distance of its 1-ring neighborhood to the final target.
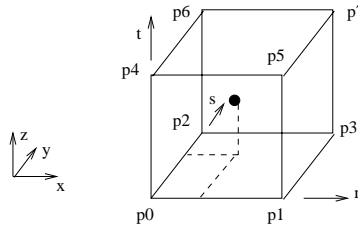
Figure 7. Parametric coordinate system for a voxel where one scalar distance value is stored at every corner

2.6. Matching the M-R Model onto a New Image

One can take advantage of the parameterized M-R representation of the reference atlas to match it onto new scans. First of all we need to register globally the coarse representation of our surface model onto the new target image. We translate the surface model so that its center matches the center of the target object in the new image. To refine this matching, we apply to the surface model an affine transform (translation, rotation and/or scaling) that minimizes a distance measure to the target object.[19] This fine automatic matching is based on the minimization of a 3D euclidean distance function between the two surfaces.

Then we propose to use the normal displacements of the M-R reference model to help the matching onto the new target image. Note that refining the model brings a finer parameterization but does not modify the geometry of the surface model. The geometry information at each resolution is represented by the normal displacements. This M-R apriori information given by the reference model can avoid the surface to match wrong edges. Hence our surface matching algorithm can address the matching onto images with an imperfect segmentation.

Finally we allow local deformation of the nodes to get the best fit to the image at the current resolution. Similarly to the building of the reference M-R surface, we iterate these operations to match the image at the full resolution.

3. EXPERIMENTAL RESULTS

In this section we report some results obtained when applying our method to brain MRI images. Our objective is to extract a surface representation of the cortex from the segmented images. To benefit from a convenient 3D image processing and visualization environment, we implemented our algorithm within the Visualization Toolkit.[18]

We encountered a situation where two regions of the surface got flattened onto each other due to a wrong matching at a low resolution. We explain this problem as follows. Due to the many folds in the inside region of the brain, the distance function only takes small values. Therefore where the deformable surface happens to enter slightly into the brain volume, it can get attracted by certain folds. Once the surface is trapped, successive surface refinement will make the surface to fold into itself. To avoid surface degeneracies, we pre-process the segmented image with a morphological closing. Hence the folds whose cross-section is smaller than the size of the structuring element vanish. We selected a one voxel-wide structuring element to only remove the smallest folds in the segmented image.

Figure 8 shows our surface model of the cortex surface rendered at three increasing resolutions. One can see the progressive appearance of the details in the surface representation from coarse to fine. The first surface (figure 8(a)) gives a coarse approximation of the 3D shape. On the second surface (figure 8(b)) more information about the geometry of the brain can be seen. The third surface (figure 8(c)) gives the full resolution representation we obtain with our M-R algorithm. For comparison purposes, the iso-surface extracted by the Marching Cubes algorithm[14] is rendered in figure 8(d). One can note the smoothness of our surface relative to the voxelized aspect of the Marching Cubes mesh. The internal force, responsible for this visually pleasing effect, leads to a representation closer to the true geometry of the brain.
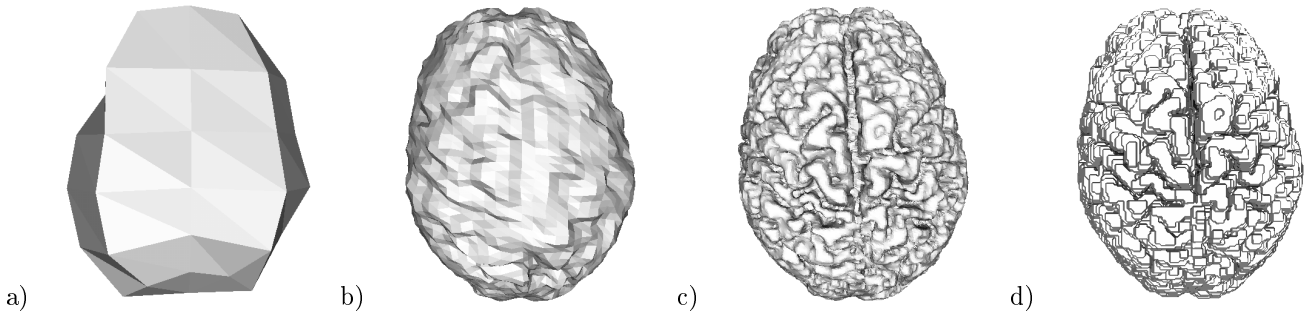

a)   b)   c)   d)
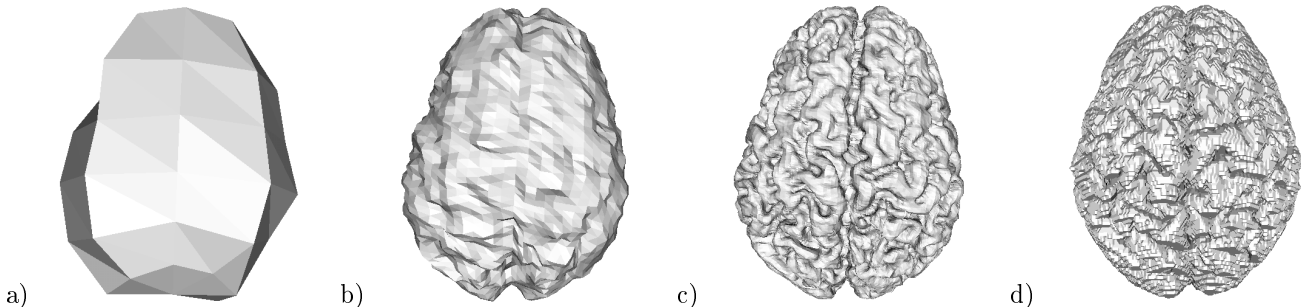
Figure 8. (a-b-c) M-R surfaces of the brain at resolution 0, 3 and 6 respectively (d) Marching Cubes mesh of the corresponding image. (flat shading used to enhance the triangulated model)

We matched this reference surface model of the brain onto a new brain MRI. Three matched surfaces are rendered in figure 9 at identical resolutions as figure 8. When comparing the representation of the two brains at a given resolution, one can observe that these surfaces exhibit information at an identical level of approximation while effectively matching the new brain image. This observation proves the coherence of our M-R representations for a given anatomical structure.

Furthermore M-R model apparently leveraged the apriori information of the reference model to adapt the slightly different geometry of the target in a M-R fashion. This observation leads to the following statement. Thanks to its wavelets-like construction, our M-R model can capture modifications of the 3D structure in a both spectrally and spatially localized way.

Figures 10 and 11 show cuts through the matched surface of figure 9 overlaid on the corresponding coronal, saggital and axial views of the 3D brain image. Figure 10 represents the lowest resolution surface (figure 9(a)) and shows the smooth approximation of the cortex shape. The cuts depicted in figure 11 illustrate the precision of our algorithm on brain images. Comparing the resolutions of figures 10 and 11, one can see that the surface enters the folds as the resolution increases. However the surface model does not still match perfectly the bottom of the brain folds. The explanation is that our distance function is computed from a morphologically closed image. In the hypothesis of a perfect distance function, one would need to further refine the surface model or lower the internal forces at the last resolutions to capture the finest details of the image.

a)   b)   c)   d)

Figure 9. (a-b-c) M-R reference surfaces of figure 8 matched onto a new image of a brain (d) Marching Cubes mesh of the corresponding image. (flat shading used to enhance the triangulated model)
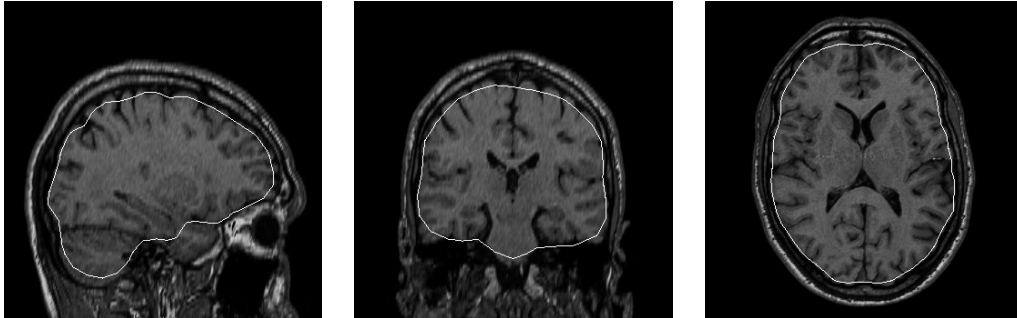

Figure 10. Cuts through lowest resolution surface model of figure 9(a) *(white outline)* overlaid on corresponding cuts through target image data

4. DISCUSSIONS AND PERSPECTIVES

While the results shown above are encouraging, our method suffers from some problems. First a morphological closing with a small structuring element was needed to get a good potential function of the image. This leads to the disadvantage that the surface cannot enter as deep as it should into the folds. In order to solve this problem, we are looking into an improved expression of this functional.

Moreover since the smoothing occurs in the deformation direction, it can affect the matching process leading to a difficult balance between the external force and the internal force. We need a fine tuning during the construction of the reference model to find a reasonable balance. Fortunately we can reuse the same tuning parameters for the matching onto a new target. Note that this tuning is less critical for matching onto new targets since the convergence is already partially achieved by the reference surface.

Our M-R method could benefit from adaptive refinement, where regions with high variations are refined with higher priority than smooth regions of the image. This lowers both the computation and the memory storage to
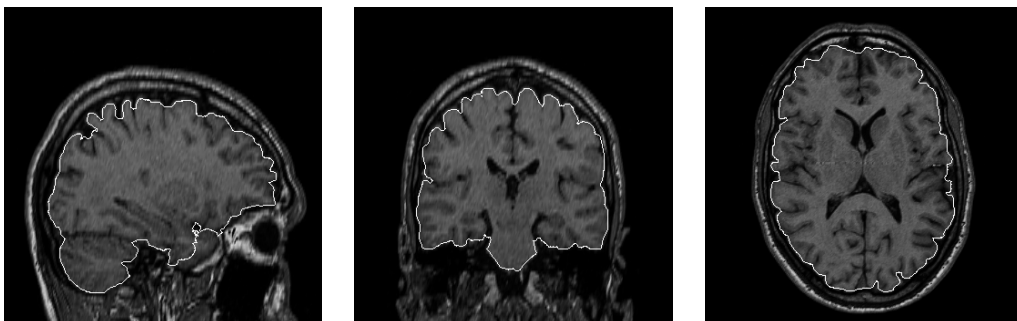
Figure 11. Same as figure 10 for the highest resolution surface model of figure 9(c)

get a surface model of equivalent quality. However one should trade off the benefits of adaptive refinement with the increased complexity of the matching process. The extraction and modification of the geometrical parameters resolution per resolution will also be problematic.

The apriori information of the surface model opens the perspective of segmenting noisy images with missing parts. The progressive matching of the reference surface will lead to a coherent segmentation that does not exhibit holes where data is missing but rather use the reference model geometry. Thanks to its spherical topology, our surface model can be mapped to a sphere to help visualization of the brain folds. Therefore a flattened brain atlas could be built allowing the automatic labeling of sulci.

Thanks to its valuable semi-regular structure, the matched M-R meshes allows for many algorithms such as progressive visualization, simplification, edition, mesh morphing, or data compression. Our M-R surface model can be used for fast visualization and progressive transmission of meshes over the network. The surface geometry can be transmitted to the user starting with the lowest resolution. This gives an approximation of the shape of the object and allows the user to have a fast rendering of the surface. When smaller details are requested by the user, the surface can be selectively refined in the regions of interest. Only one displacement scalar per node needs to be transmitted to reconstruct the surface at the next resolution.

5. CONCLUSIONS

We have presented a new algorithm for automatic Multi-Resolution surface registration. This algorithm starts from a low triangle count surface model that gets iteratively refined and matched onto the image. The surface is locally deflated or inflated to minimize an euclidean distance measure while preserving global smoothness. As resolution increases this model is refined by triangle quadrisection to match image details on a smaller scale. Matching the surface from coarse to fine improves both convergence and precision of the deformation in comparison with classical active-surface algorithms. Finally the geometric information of the reference model is used resolution per resolution to guide the matching of this model onto new images. We have shown promising results of our algorithm for the matching of the cortical surface in brain MRI images.

ACKNOWLEDGMENTS

REFERENCES

1. S. Angenent, S. Haker, A. Tannenbaum, and R. Kikinis, "Conformal geometry and brain flattening," in *MICCAI 99: Second International Conference on Medical Image Computing and Computer-Assisted Intervention; October 1999; Cambridge, England.*, pp. 271–278, September 1999.
2. T. McInerney and D. Terzopoulos, "A dynamic finite element surface model for segmentation and tracking in multidimensional medical images
   with application to cardiac 4d image analysis," *Comput. Med. Imag. Graph.* **19**, pp. 69–83, 1995.
3. P. Thompson and A. Toga, "A Surface-Based Technique for Warping Three-Dimensional Images of the Brain," *IEEE Trans. Med. Imag* **15**(4), pp. 402–417, 1996.
4. P. M. Thompson, J. N. Giedd, R. P. Woods, D. MacDonald, A. C. Evans, and A. W. Toga, "Growth patterns in the developing brain detected by using continuum mechanical tensor maps," *Nature* (404), pp. 190–193, 2000. Macmillan Publishers Ltd.
5. M. Kass, A. Witkin, and D. Terzopoulos, "Snakes: Active Contour Models," *International Journal of Computer Vision* **1**(4), pp. 321–331, 1988.
6. L. Cohen and C. I., "Finite Element Methods for Active Contour Models and Balloons for 2D and 3D Images," *IEEE Trans. Pattern Anal. and Machine Intell.* **15**, pp. 1131–1147, 1993.
7. M. Ferrant, O. Cuisenaire, and B. Macq, "Multi-Object Segmentation of Brain Structures in 3D MRI Using a Computerized Atlas," in *SPIE Medical Imaging '99*, vol. 3661-2, pp. 986–995, 1999.
8. C. Xu and J. L. Prince, "Snakes, shapes, and gradient vector flow," *IEEE Transactions on Image Processing* **7**, pp. 359–369, March 1998.
9. C. Davatzikos, "Spatial Transformation and Registration of Brain Images Using Elastically Deformable Models," *Computer Vision and Image Understanding* **66**, pp. 207–222, May 1997.

10. B. Leroy, I. L. Herlin, and L. D. Cohen, "Multi-resolution algorithms for active contour models," in *12th Int. Conf. Analysis and Optimization of Systems*, pp. 58–65, 1996.

11. I. Daubechies, I. Guskov, P. Schröder, and W. Sweldens, "Wavelets on irregular point sets," *Phil. Trans. R. Soc. Lon. A.* **357**(1760), pp. 2397–2413, 1999.

12. I. Guskov, W. Sweldens, and P. Schröder, "Multiresolution signal processing for meshes," *Computer Graphics Proceedings (SIGGRAPH 99)* , pp. 325–334, ACM Siggraph, 1999.

13. Z. Wood, M. Desbrun, P. Schröder, and D. Breen, "Semi-regular mesh extraction from volumes," in *ACM Proceedings of Visualization*, 2000.

14. W. Lorensen and H. Cline, "Marching Cubes: a High Resolution 3D Surface Construction Algorithm," in *Computer Graphics (SIGGRAPH '87)*, vol. 21, pp. 163–169, 1987.

15. I. Guskov, K. Vidimce, W. Sweldens, and P. Schröder, "Normal meshes," in *Computer Graphics Proceedings, ACM SIGGRAPH*, pp. 95–102, 2000.

16. J. Thiran, V. Warscotte, and B. Macq, "A Queue-based Region Growing Algorithm for Accurate Segmentation of Multi-Dimensional Images," *Signal Processing* **60**, pp. 1–10, 1997.

17. O. Cuisenaire and B. Macq, "Fast Euclidean Distance Transformation by Propagation Using Multiple Neighborhoods," *Computer Vision and Image Understanding* **76**, pp. 163–172, November 1999.

18. W. Schroeder, K. Martin, and B. Lorensen, *The Visualization Toolkit: An Object-Oriented Approach to 3D Graphics*, Prentice Hall PTR, New Jersey, second ed., 1998.

19. O. Cuisenaire, J. Thiran, B. Macq, C. Michel, A. De Volder, and F. Marques, "Automatic Registration of 3D Images with a Computerized Brain Atlas," in *SPIE Medical Imaging '96*, SPIE, ed., vol. 1719, pp. 438–449, 1996.